THE JOURNAL OF BIOLOGICAL CHEMISTRY VOL. 283, NO. 50, pp. 34913–34922, December 12, 2008


# Ryanodine Receptor Activation by $Ca_v1.2$ Is Involved in Dendritic Cell Major Histocompatibility Complex Class II Surface Expression*

Received for publication, June 11, 2008, and in revised form, October 10, 2008 Published, JBC Papers in Press, October 16, 2008, DOI 10.1074/jbc.M804472200

**Mirko Vukcevic[‡], Giulio C. Spagnoli[§], Giandomenica Iezzi[§], Francesco Zorzato[¶], and Susan Treves[‡1]**

*From the [‡]Departments of Anaesthesia and Biomedicine and [§]Institute of Surgical Research, Basel University Hospital, 4031 Basel, Switzerland and the [¶]Department of Experimental and Diagnostic Medicine, General Pathology section, University of Ferrara, 44100 Ferrara, Italy*

**Dendritic cells express the skeletal muscle ryanodine receptor (RyR1), yet little is known concerning its physiological role and activation mechanism. Here we show that dendritic cells also express the $Ca_v1.2$ subunit of the L-type $Ca^{2+}$ channel and that release of intracellular $Ca^{2+}$ via RyR1 depends on the presence of extracellular $Ca^{2+}$ and is sensitive to ryanodine and nifedipine. Interestingly, RyR1 activation causes a very rapid increase in expression of major histocompatibility complex II molecules on the surface of dendritic cells, an effect that is also observed upon incubation of mouse BM12 dendritic cells with transgenic T cells whose T cell receptor is specific for the I-$A^{bm12}$ protein. Based on the present results, we suggest that activation of the RyR1 signaling cascade may be important in the early stages of infection, providing the immune system with a rapid mechanism to initiate an early response, facilitating the presentation of antigens to T cells by dendritic cells before their full maturation.**

$Ca^{2+}$ signals regulate a variety of functions in eukaryotic cells from muscle contraction and neuronal excitability to gene transcription, cell proliferation, and cell death. To efficiently utilize $Ca^{2+}$ as a second messenger, cells are equipped with an essential toolbox kit composed of a variety of proteins that allow $Ca^{2+}$ ions to flow into the cytoplasm and be removed from the cytoplasm, proteins that store/buffer $Ca^{2+}$ in intracellular organelles, and proteins acting as sensors for intracellular $Ca^{2+}$ levels as well as $Ca^{2+}$-regulated enzymes (1, 2). In both excitable and non-excitable cells, generation of an intracellular $Ca^{2+}$ transient is due to the release of $Ca^{2+}$ from intracellular stores via inositol 1,4,5-trisphosphate or ryanodine receptors (RyRs)[2] present on the endoplasmic (ER)/sarcoplasmic reticulum membranes and opening of $Ca^{2+}$ channels present on the plasma membrane. Both the amplitude and the frequency of the $Ca^{2+}$ signal can be sensed by specific proteins allowing a cell to respond appropriately to signals, which apparently only give rise to an increase in the intracellular $Ca^{2+}$ concentration ($[Ca^{2+}]_i$). In general, non-excitable cells are endowed with inositol 1,4,5-trisphosphate receptors which open in response to the generation of the receptor coupled second messenger inositol 1,4,5-trisphosphate, allowing $Ca^{2+}$ to flow out of the ER. On the other hand, excitable cells, which need to respond to signals within milliseconds, are equipped with RyR $Ca^{2+}$ channels (1). Regulation of the latter class of proteins is not mediated by the generation of a second messenger but rather through coupling with another protein component present on the plasma membrane, the L-type $Ca^{2+}$ channel (3). In fact, in cardiac and skeletal muscles, signaling to the RyR is coupled to the dihydropyridine receptor (DHPR) L-type $Ca^{2+}$ channels, which sense changes in membrane potential thereby activating $Ca^{2+}$ release from the sarcoplasmic reticulum. L-type $Ca^{2+}$ channels are composed of an $\alpha 1$ subunit ($Ca_v$), which spans the membrane and contains the pore region, and the four additional subunits $\beta 1$, $\alpha 2$, $\gamma$, and $\delta$. There are at least four genes encoding the $\alpha 1$ subunits ($Ca_v1.1$-$Ca_v1.4$), and all mediate L-type $Ca^{2+}$ currents, although their products are preferentially expressed in different tissues/subcellular locations (3, 4). $Ca_v1.1$ is localized in the transverse tubules and is involved in skeletal muscle excitation-contraction coupling; $Ca_v1.2$ is expressed in cardiac and smooth muscle cells, endocrine cells, and pancreatic $\beta$ cells as well as in neuronal cell bodies and is involved in cardiac excitation-contraction coupling, hormone release, transcription regulation, and synaptic integration. $Ca_v1.3$ and $Ca_v1.4$ have a more widespread distribution, including neuronal cell bodies, dendrites, pancreatic $\beta$ cells, cochlear hair cells, adrenal gland, and mast cells where they are involved in hormone/neurotransmitter release, regulation of transcription, and synaptic regulation (4).

Ryanodine receptors belong to a family of intracellular $Ca^{2+}$ release channels composed of at least three different isoforms that have been characterized extensively biochemically, functionally, and at the molecular level (5–7). Type 1 RyRs are

* This work was supported by Swiss National Science Foundation Grants 3200B0-114597, 31600-117383 and 3200B0-104060 and by Swiss Muscle Foundation and Association Française Contre les Myopathies. The costs of publication of this article were defrayed in part by the payment of page charges. This article must therefore be hereby marked "*advertisement*" in accordance with 18 U.S.C. Section 1734 solely to indicate this fact.

[1] To whom correspondence should be addressed: Depts. of Anesthesia and Biomedical Research, Basel University Hospital, Hebelstrasse 20, 4031 Basel, Switzerland. Tel.: 41-61-2652373; Fax: 41-61-2653702; E-mail: susan.treves@unibas.ch.

[2] The abbreviations used are: RyR, ryanodine receptor; MHC, major histocompatibility complex; $[Ca^{2+}]_i$, intracellular calcium concentration; DC, dendritic cell; iDC, immature DC; DHPR, dihydropyridine receptor; ER, endoplasmic reticulum; LPS, lipopolysaccharide; bis-oxonol, bis-(1,3-diethylthiobarbiturate)-trimethineoxonal; PBS, phosphate-buffered saline; FITC, fluorescein isothiocyanate; PE, phycoerythrin; Abs, antibody; HLA, human leukocyte antigens; ABM, anti-BM12.

encoded by a gene on human chromosome 19 and are mainly expressed in skeletal muscle and to a lower extent in Purkinje cells. Mutations in this gene are associated with the rare neuromuscular disorders malignant hyperthermia, central core disease, and some forms of multiminicore disease (8, 9). Type 2 RyR is mainly expressed in cardiac muscles and cerebellum. Mutations in its gene are associated with genetic variants of congestive heart failure, namely catecholaminergic polymorphic ventricular tachycardia and arrhythmogenic right ventricular dysplasia (10, 11). Type 3 RyRs are expressed in a variety of excitable tissues as well as in immature muscle cells (12). Recent reports have demonstrated that type 1 RyRs are also expressed in some cells of the immune system (13), particularly B-lymphocytes and dendritic cells (DCs) where their pharmacological activation gives rise to a rapid and transient increase in the intracellular $Ca^{2+}$ concentration (14–19).

Although both B-lymphocytes and DCs can act as antigen presenting cells and initiate T cell-driven immune responses (20), DCs play a central role in the immune system; they are strategically located in peripheral tissues where they continuously sample their environment for the presence of antigens. Upon encounter with microbial products or tissue debris, immature DCs (iDCs) stop endocytosing, undergo maturation, and become the most potent antigen presenting cells known. Mature DCs up-regulate co-stimulatory molecules and antigen-presenting molecules, transcribe mRNA for specific cytokines, and migrate to secondary lymphoid organs where they interact with naïve T cells to initiate specific immune responses (21). Complete maturation of DCs is thought to require at least 10–20 h (22, 23). The involvement of $Ca^{2+}$ signaling events in DC maturation had been postulated for a number of years, but only recently was it demonstrated that RyR1-mediated $Ca^{2+}$ signals can act synergistically with signals generated via Toll-like receptors driving DC maturation (17, 19). Experimentally, iDCs can be induced to undergo maturation by treatment with high ($\mu$M) concentrations of lipopolysaccharide. Physiologically, however, an inflamed region most likely contains a mixture of bacterial components, tissue and cellular debris, and other cellular components, including ions released from dying cells.

Several questions emerge concerning the role(s) of RyRs in DCs. (i) Why do these cells utilize the rapid acting RyRs to achieve such a slow process such as maturation; are RyRs involved in other aspects of DC function? (ii) What is the physiological route of RyR1 activation in DCs? In skeletal muscle the $Ca_v1.1$ subunit of the DHPR L-type $Ca^{2+}$ channel present on the transverse tubular membrane acts as a voltage sensor and interacts directly with the RyR1 to initiate $Ca^{2+}$ release. Are DCs equipped with a similar signaling pathway?

In the present report we show that DCs are endowed with a DHPR which is activated by membrane depolarization and triggers $Ca^{2+}$ release via RyR1. More importantly we show that activation of this signaling pathway is both necessary and sufficient to cause the rapid release of an intracellular pool of MHC class II molecules onto the plasma membrane. We hypothesize that a such a rapid signaling machinery may be important under specific conditions, namely in the very early phases of an immune response when T cells and iDCs may become intimately connected; engagement of T cell receptors with the MHC class II molecules on the surface of iDCs rapidly activates T cells to release factors stimulating an increase in the level of expression of MHC class II molecules on the surface of iDCs, possibly supporting very early activation steps of T cells.

## EXPERIMENTAL PROCEDURES

*Isolation and Generation of Dendritic Cells*—Human iDCs were generated from peripheral blood mononuclear leukocytes as previously described (17). Briefly monocytes were purified by positive sorting using anti-CD14 conjugated magnetic microbeads (Miltenyi Biotech, Bergisch Gladbach, Germany). Sorted monocytes were cultured for the following 5 days in differentiation medium containing RPMI, 10% fetal calf serum, glutamine, nonessential amino acids, and antibiotics (Invitrogen) supplemented with 50 ng/ml granulocyte-macrophage colony-stimulating factor (Laboratory Pablo Cassarà, Buenos Aires, Argentina) and 1000 units/ml interleukin 4 (a gift from A. Lanzavecchia, Bellinzona, Switzerland).

Murine dendritic cells were isolated by positive sorting from spleens treated with collagenase D (1 mg/ml; Worthington Biotech; Lakewood, NJ) using anti-CD11c-coated magnetic MicroBeads according to the manufacturer's instructions (Miltenyi Biotech). The phenotype of cells was evaluated before experiments by flow cytometry using a FACSCalibur instrument equipped with Cell Quest software (BD Biosciences) as previously described (17).

*Preparation of Necrotic Cell Extracts*—Extracts were prepared essentially as described (17); briefly, cultured HEK293 cells ($1–1.5 \times 10^7$) were harvested, rinsed twice with PBS, resuspended in PBS, and subjected to 5 cycles of freeze-thawing. Viability was assessed by trypan blue exclusion and was <5%. Large cellular debris were removed by centrifugation, and their supernatant was filtered twice through a 0.22-$\mu$m Millipore filter and stored at −70 °C. Where indicated, extracts were dialyzed overnight at room temperature against PBS using a 3000 Da cut-off Spectrapore dialysis membrane (Spectrum Laboratories). Extracts were then centrifuged and filtered twice through 0.22-$\mu$m Millipore filters.

*Stimulation of iDC and CD83 Expression—In vitro* derived iDCs were cultured for 4 h at 37 °C in the presence of 1 $\mu$g/ml LPS (from *Salmonella abortus* equi, Sigma) or in the presence of 1 ng/ml LPS supplemented with supernatants from necrotic cells. Briefly, necrotic cell extracts obtained from $1 \times 10^7$ cells (1.2 ml) were added to $0.8 \times 10^6$ iDCs cultured in 1 ml of differentiation medium plus 1 ng/ml LPS; when nifedipine or dantrolene were used iDCs were pretreated at 37 °C for 45 min in the dark with 10 $\mu$M nifedipine (Calbiochem) or 20 $\mu$M dantrolene (Sigma) before the addition of the necrotic extract. Cells were harvested, and surface expression of CD83 was investigated by flow cytometry using FITC-labeled anti-CD83 monoclonal antibodies (BD Pharmingen) on paraformaldehyde (1% in PBS) fixed cells.

*Single-cell Intracellular $Ca^{2+}$ Measurements*—Measurements were performed on fura-2 (Molecular Probes, Eugene, OR)-loaded iDCs. In some experiments fura-2 loading and incubation with 500 $\mu$M ryanodine (Calbiochem) were performed simultaneously. After loading, cells were rinsed once,

resuspended in Krebs-Ringer medium and allowed to adhere to glass coverslips, which were then mounted onto a 37 °C thermostatted chamber that was continuously perfused with Krebs-Ringer medium containing 1 mM $CaCl_2$. Individual cells were stimulated with the indicated agonist by way of a 12-way 100-mm diameter quartz micromanifold computer-controlled microperfuser (ALA Scientific, Westbury, NY) as previously described (15). Online (340 nm, 380 nm, and ratio) measurements were recorded using a fluorescent Axiovert S100 TV inverted microscope (Carl Zeiss, Jena, Germany) equipped with a 40× oil immersion Plan Neofluar objective (0.17 NA) and filters (BP 340/380, FT 425, BP 500/530) and attached to a Hamamatsu multiformat CCD camera. Cells were analyzed using an Openlab imaging system, and the average pixel value for each cell was measured at excitation wavelengths of 340 and 380 nm, as previously described (15).

*Membrane Potential Measurements*—Changes in membrane potential were assessed after the changes in fluorescence of the lipophilic dye bis-(1,3-diethylthiobarbiturate)-trimethineoxonal (bis-oxonol) as described by the manufacturer (Molecular Probes). iDCs ($0.65 \times 10^6$ cells/ml) were rinsed, resuspended in PBS, and added to a cuvette containing 200 nM bis-oxonol in PBS. After allowing the dye to equilibrate, changes in fluorescence were monitored with a PerkinElmer Life Sciences LS50 spectrofluorometer equipped with magnetic stirrer and thermostatted at 37 °C.

*Immunofluorescence Analysis*—Immunofluorescence analysis was performed as indicated on methanol-fixed or methanol: acetone (1:1)-fixed iDCs using rabbit anti-$Ca_v1.2$ antibody (anti-CCAT, a gift from Natalia Gomez-Ospina and Prof. Ricardo Dolmetsch, Department of Neurobiology, Stanford University School of Medicine, Stanford CA), goat anti-RyR (Santa Cruz Biotechnology Inc.), mouse anti-human HLA DR (Caltag Laboratories, Burlingame CA) followed by Alexa Fluor-488-conjugated chicken anti-rabbit IgG, Alexa Fluor-555-conjugated donkey anti-goat IgG (Molecular Probes), or PE-conjugated goat anti-mouse IgG (Southern Biotech). Fluorescence was visualized using a 100× Plan NEOFLUAR oil immersion objective (NA 1.3) mounted on a Zeiss Axiovert 100 as previously described (17).

*Immunoblotting and Reverse Transcription PCR Analysis*—For Western blots iDCs ($1 \times 10^7$ cells) were washed 3 times with PBS, and the pellet was then resuspended in 500 μl of detergent extraction buffer containing 1% Nonidet, 0.5% sodium deoxycholate, 150 mM NaCl, 5 mM EDTA, 50 mM Tris-HCl, pH 8.0, plus anti-proteases (EDTA-free, Roche Applied Science), passed through a 25-gauge needle, and incubated for 5 min at 95 °C. The solubilized proteins from $1 \times 10^6$ cells were loaded in each lane and separated on a 6% SDS-PAG. Proteins were transferred onto nitrocellulose, and the blots were probed with a rabbit anti-$Ca_v1.2$ antibody (1:2000) followed by peroxidase-conjugated protein G (1:50000. Fluka Biochemicals, Buchs, Switzerland). The immunopositive bands were visualized by autoradiography using the Super signal West Dura chemiluminescence kit from Thermo Scientific.

Reverse transcription PCR was performed as previously described (15). Total RNA was isolated from $8 \times 10^6$ iDCs using the ULTRASPEC RNA isolation system (Biotex Labs) and reverse-transcribed using a cDNA synthesis kit following the instructions provided by the manufacturer (Roche Applied Science). Approximately 100 ng of cDNA were used per PCR amplification using an Applied Biosystems 2720 thermal cycler. The following primers spanning exons 15–16 were used to amplify the $Ca_v1.2$ transcript: forward, 5′-AAA TTT CCCT GGG ACTG TTG; reverse, 5′-GGT TAT GCCC TCCC CTG. Such primers yield a DNA fragment of ~300 bp when amplifying cDNA; amplification from genomic DNA would be highly unlikely under normal PCR conditions as the expected fragment is too large (~2800 bp). Amplification conditions were 5 min at 95 °C followed by 35 cycles of 30 s annealing at 92 °C, 40 s extension at 50 °C, and 40 s denaturation at 72 °C followed by a final extension for 5 min at 72 °C using the 2.5× Master Mix Taq polymerase from Eppendorf. The products of the PCR reaction were separated on a 6% polyacrylamide gel, and the bands were visualized by ethidium bromide staining.

*Functional Properties of iDCs*—Endocytosis was studied by incubating iDCs in RPMI medium containing FITC-labeled dextran (final concentration 0.5 mg/ml; Fluka Chemicals, Buchs, Switzerland) for 30 min at 37 °C. Cells were washed in ice-cold PBS 2 times and fixed with 1% paraformaldehyde, and the number of FITC-positive cells was assessed by flow cytometry.

Surface expression of MHC class I and class II molecules was monitored in iDCs stimulated with 10 mM caffeine for 1–60 min at 37 °C or on iDCs stimulated with 100 mM KCl, necrotic cell extracts, 100 μM ATP, or 1 μg/ml LPS for 1 min. To monitor surface expression of MHC class I and II molecules, stimulated cells were washed with ice-cold PBS, labeled, and analyzed by flow cytometry using FITC-labeled anti-human HLA DR and HLA A, B, C or, in the case of mouse CD11c+ cells, with FITC-labeled anti mouse $I\text{-}A^b$ monoclonal antibody (BD Pharmingen).

*In Vivo Investigation of Mouse DC-T cell Interactions; Increase in $[Ca^{2+}]_i$ and Rapid MHC Class II Induction*—CD11c positive DCs were isolated from the spleens of either B6.C-H-2bm12Ly 5.1 mice (abbreviated BM12DC) or B6.Ly 5.1 mice (a generous gift of Prof. Ed Palmer, Department of Biomedicine, Basel University Hospital, Basel, Switzerland). T-lymphocytes were isolated from the lymph nodes of ABM $Rg^{-/-}$ mice. These T cells recognize the $I\text{-}A^{bm12}$ protein expressed on the surface of B6.C-H-2bm12.Ly5.1 DCs but do not recognize the $I\text{-}A^b$ protein expressed on the surface of B6.Ly5.1 DCs (24). T-lymphocytes were divided in two groups; one group was left untreated, whereas the other was incubated with 100 nM charybdotoxin (Alexa Biochemicals) for 45 min to block $K^+$ channels (25), after which the cells were washed to remove excess toxin.

For $Ca^{2+}$ imaging BM12DC were loaded with the fluorescent $Ca^{2+}$ indicator fluo-4 AM (Invitrogen; 5 μM final concentration) for 60 min at 37 °C. In some experiments BM12DCs were simultaneously incubated with 500 μM ryanodine (Calbiochem) and fluo-4 AM. Cells were then washed and resuspended in Krebs-Ringer containing 1 mM $CaCl_2$ and 0.2% bovine serum albumin. BM12DC were allowed to adhere to glass coverslips which were then mounted on a 37 °C thermostatted chamber. Experiments were started by adding T-lymphocytes to the coverslip onto which the BM12DCs had been applied. Changes in

fluo-4 fluorescence were monitored with a Nikon Eclipse TE2000-E fluorescent microscope equipped with a CFI APO TIRF 60× objective. Changes in fluorescence were detected by exciting at 488 nm and recording the emission at 510-nm via an electron multiplier C9100–13 Hamamatsu CCD camera. Image analysis was performed with the MetaMorph (Molecular Devices) analysis software package.

For MHC II induction untreated T-lymphocytes or T-lymphocytes preincubated with 100 nM charybdotoxin (Alexa Biochemicals) for 45 min and washed to remove excess toxin were used. Both batches of T cells were placed in 1.5-ml Eppendorf tubes together with the CD11c positive B6 or B6.C-H-2bm12 DCs. Cells were spun down for 30 s using a Tomy PMC-060 capsulefuge and incubated at 37 °C for an additional 5 min. They were then diluted with ice-cold PBS, washed, and labeled with FITC-anti-mouse I-$A^b$, biotin-labeled anti-CD11c plus APC (allophycocyanin)-labeled streptavidin, and PE-labeled anti-CD45.1 (all from BD Pharmingen). Expression of MHC class II molecules was determined on triple positive cells by flow cytometry.

*Statistical Analysis and Software Programs*—Statistical analysis was performed using the Student's *t* test for unpaired samples; means were considered statistically significant when the *p* value was <0.05. The Origin computer program (Microcal Software, Inc., Northampton, MA) was used to generate graphs and for statistical analysis. Figures were assembled using Photoshop Adobe.

## RESULTS

*Upstream Events Leading to RyR1 Activation*—In an earlier report (17) we showed that (i) iDCs only express the type 1 RyR isoform, (ii) the addition of caffeine, 4-chloro-m-cresol, or KCl to iDC causes a RyR1-dependent increase in the intracellular $Ca^{2+}$ concentration ($[Ca^{2+}]_i$), and (iii) the signaling cascade activated by the $Ca^{2+}$ increase acts synergistically with signals generated via Toll-like receptors, stimulating DC maturation (17). Because RyRs are present in intracellular membranes and are not directly accessible to stimulation, our first aim was to identify events upstream from RyR1 activation by first searching for, and then using a more physiological stimulus leading to DC maturation.

Fig. 1 shows that treatment of iDCs with a suboptimal concentration of lipopolysaccharide (LPS 1 ng/ml) for 4 h in the presence of necrotic cell extracts, a stimulus that has been shown to cause maturation (26), leads to a significant increase in the surface expression of CD83, a reliable phenotypic marker for DC maturation (17, 27, 28). The signals generated by the addition of the necrotic cell extracts and leading to maturation were significantly decreased by pretreatment of cells with dantrolene ($p < 0.034$), an inhibitor of the RyR1 (29) and nifedipine ($p < 0.019$), a well known L-type $Ca^{2+}$ channel inhibitor (4). The functional involvement of a nifedipine- and ryanodine-sensitive $Ca^{2+}$ signal was confirmed by direct measurements of the intracellular $[Ca^{2+}]$ (Fig. 2, *A* and *B*). Individual fura-2 loaded iDCs were stimulated with filtered extracts from necrotic cells. This treatment caused a transient and rapid increase in $[Ca^{2+}]_i$, which was significantly decreased ($p < 0.0001$) by preincubation of iDCs with 500 μM ryanodine (Fig. 2*A*, *inset*) (at high concentrations ryanodine blocks the RyR (30, 31); dantrolene, which is used to inhibit RyR-signaling events, is fluorescent and interferes with imaging when using fluorescent $Ca^{2+}$ indicators) or 10 μM nifedipine ($p < 0.0001$; Fig. 2*A*); in fact, the mean Δ fluorescence induced by necrotic extracts was 0.210 ± 0.011 in untreated cells and 0.134 ± 0.094 and 0.029 ± 0.008 in cells pretreated with 500 μM ryanodine or 10 μM nifedipine, respectively. A similar result was observed after the addition of 100 mM KCl to iDCs (Fig. 2*B*). In the latter case, if the experiments were performed in the absence of extracellular $Ca^{2+}$ and in the presence of 100 μM $La^{3+}$ to block $Ca^{2+}$ influx (32) or on iDCs which had been pretreated with 500 μM ryanodine or 10 μM nifedipine, the mean increases in fluorescence induced by the addition of 100 mM KCl were significantly reduced (Fig. 2*B*; $p < 0.0001$), indicating that the intracellular $Ca^{2+}$ transient is dependent on the activation of the RyR1, on influx of $Ca^{2+}$ from the extracellular medium, and is sensitive to micromolar concentrations of nifedipine.

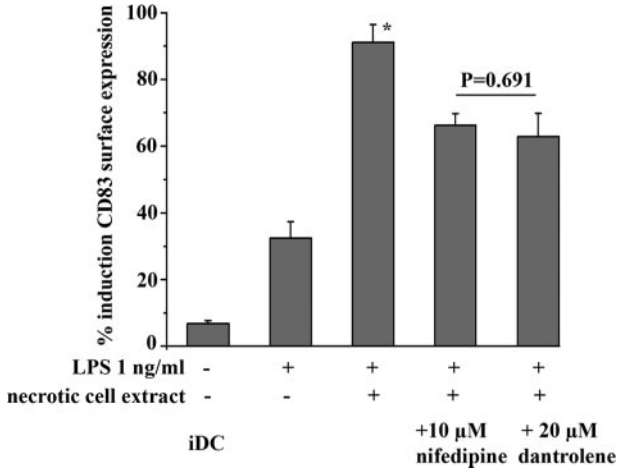


FIGURE 1. **Surface expression of CD83 induced by necrotic cell extracts is sensitive to dantrolene and nifedipine.** iDCs were treated for 4 h as indicated, and the number of positive CD83 cells was determined by flow cytometry on paraformaldehyde (1% in PBS) fixed cells. Stimulation with 1 ng/ml LPS alone induced a small increase CD83 surface expression; the concomitant presence of supernatants from necrotic HEK293 cells, prepared as described under "Experimental Procedures" increased CD83 significantly as compared with iDCs treated with 1 ng/ml LPS (*, $p < 0.02$). This effect was blocked by pretreatment of iDCs with the RyR1 inhibitor dantrolene (20 μM; $p < 0.034$) or with the L-type $Ca^{2+}$ channel inhibitor nifedipine (10 μM; $p < 0.019$). Results are expressed as the mean (±S.E.) % induction of CD83 surface expression of at least three experiments carried out on iDCs purified from blood of different donors; values obtained by treating iDCs with 1 μg/ml LPS were considered 100%.

These results suggest that KCl and necrotic cell extracts may act in a similar fashion; KCl causes membrane depolarization, and this can be followed experimentally with the fluorescent membrane potential dye bis-oxonol whereby depolarization increases the fluorescence of bis-oxonol (Fig. 2*C*, *left* and *central panels*), whereas hyperpolarization causes a decrease in fluorescence. The addition of filtered necrotic cell extracts to iDCs causes plasma membrane depolarization (Fig. 2*C*, *right panel*), and the extent of depolarization is proportional to the number of cells from which the extracts were prepared (not shown); overnight dialysis of the necrotic extract against PBS with a 3000-Da cut-off membrane abolished its depolarizing effect (Fig. 2*C*, *right panel*).

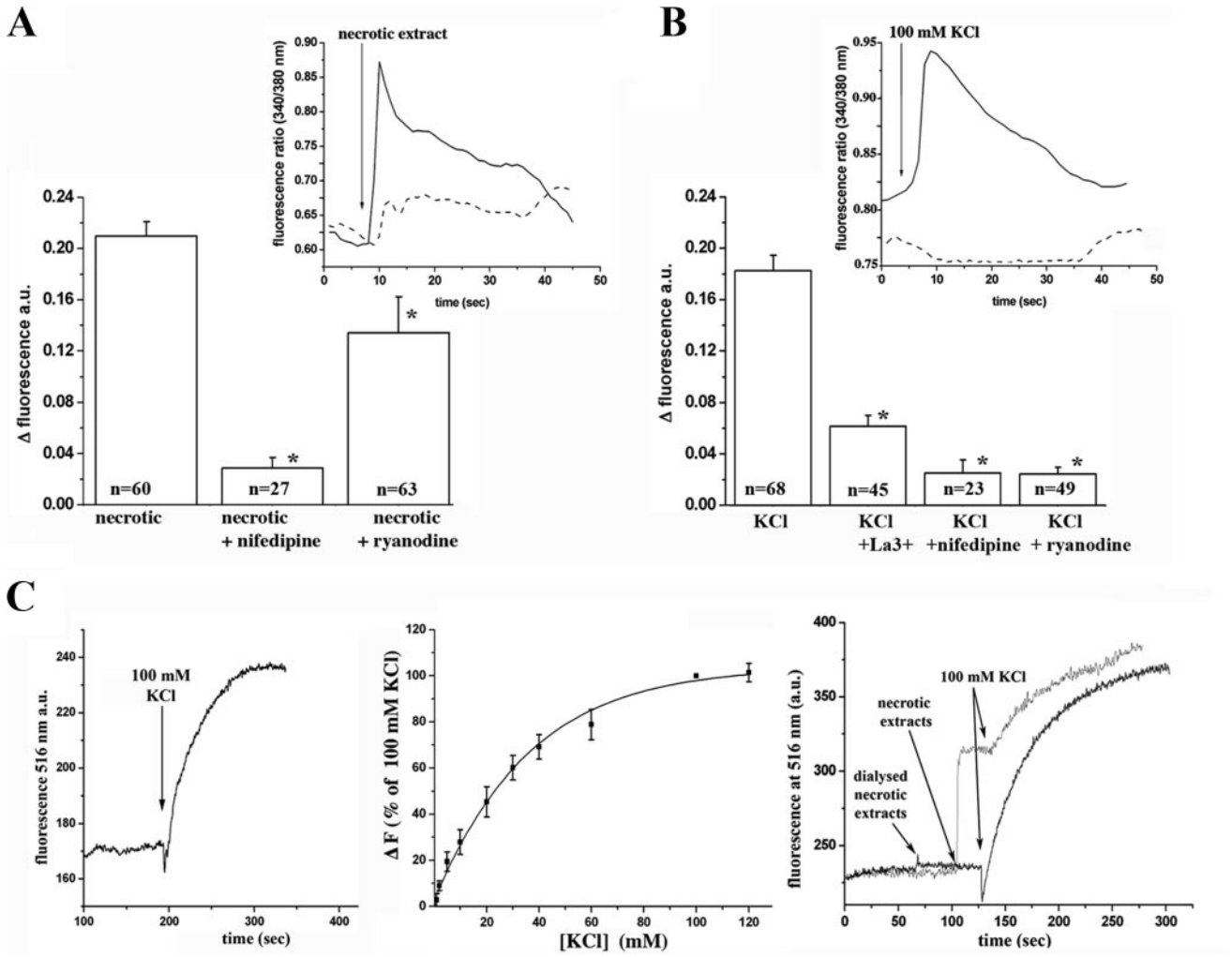


FIGURE 2. **Necrotic cell extracts and KCl induce a nifedipine-sensitive increase in $[Ca^{2+}]$ in iDCs as well as membrane depolarization.** *A* and *B*, single cell intracellular calcium measurements in fura-2-loaded iDCs. The *traces* in the *insets* show changes in the fura-2 fluorescence ratio (340/380 nm) in single iDC perfused with necrotic cell extracts (*A*) or 100 mM KCl (*B*) *Continuous line*, no pretreatment; *dashed line*, cells pretreated with 500 $\mu$M ryanodine for 60 min. Experiments were performed in Krebs-Ringer containing 1 mM $Ca^{2+}$ except when $La^{3+}$(100 $\mu$M) was added, in which case only contaminating $Ca^{2+}$ was present. When nifedipine or ryanodine were used, cells were preincubated with 10 $\mu$M nifedipine or 500 $\mu$M ryanodine during the fura-2 loading. The histograms represent the mean (±S.E. of the indicated n values) Δ increase in fluorescence, calculated by subtracting the peak fluorescence ratio−resting fluorescence ratio): *, $p < 0.0001$. *C*, membrane potential changes were monitored by following the change in fluorescence of bis-oxonol as detailed under "Experimental Procedures." After allowing the dye to equilibrate, either KCl or filtered necrotic extracts obtained from $2.9 \times 10^6$ cells were added to the cuvette while continuously monitoring the emission at 516 nm. An upward deflection indicates membrane depolarization. Experiments were carried out at least three times giving similar results. The mean (±S.E.) of 4–6 values were used to generate the Δ fluorescence-KCl dose-dependent curve shown in *panel C* (*center*). *a.u.*, arbitrary units.

In cardiac and skeletal muscles, signaling to the RyR1 is coupled to DHPR L-type $Ca^{2+}$ channels, which sense changes in membrane potential thereby activating $Ca^{2+}$ release from the sarcoplasmic reticulum. Because human iDCs express the $\beta$1 subunit of the DHPR (33), we wondered whether the depolarization-coupled $Ca^{2+}$ release observed in iDC could be due to the expression of a $Ca_v1$ isoform by these cells. Immunofluorescence analysis using confocal microscopy on methanol-fixed iDCs labeled with anti-$Ca_v1.2$ Abs followed by Alexa Fluor-488-conjugated anti-rabbit IgG (Fig. 3*A*, *panel 1*) and anti-MHCII Abs (Fig. 3*A*, *panel 2*) followed by PE-conjugated anti-mouse IgG confirmed partial co-localization of the two proteins on the plasma membrane of iDCs (Fig. 3*A*, *panel 5*). We next verified if there was co-localization between $Ca_v1.2$ and the RyR by performing immunofluorescence analysis on permeabilized acetone-methanol-fixed iDCs. Under these conditions $Ca_v1.2$ appeared to be discretely distributed within iDCs (Fig. 3*B*, *panel 1*), whereas immunostaining for the RyR1 showed a more reticular pattern of distribution (Fig. 3*B*, *panel 2*); merging the two images shows that part of the positive fluorescent signals obtained with anti-$Ca_v1.2$ and anti-RyR overlap (Fig. 3*B*, *panel 5*), indicating that the two proteins co-localize within certain domains of iDCs. To confirm that the antibodies recognize a protein corresponding to $Ca_v1.2$, we performed Western blot analysis. Fig. 3*C* shows that the anti-$Ca_v1.2$ Abs we used, which were specifically raised against the COOH terminus of $Ca_v1.2$ (34), recognize a band in total iDC extracts migrating with an apparent molecular mass of 200 kDa as well as another immunopositive band with a slightly slower mobility; very similar results were obtained by Gomez-Ospina who used these Ab to identify $Ca_v1.2$ in neurons (34). Finally, reverse transcription-PCR using primers specifically designed

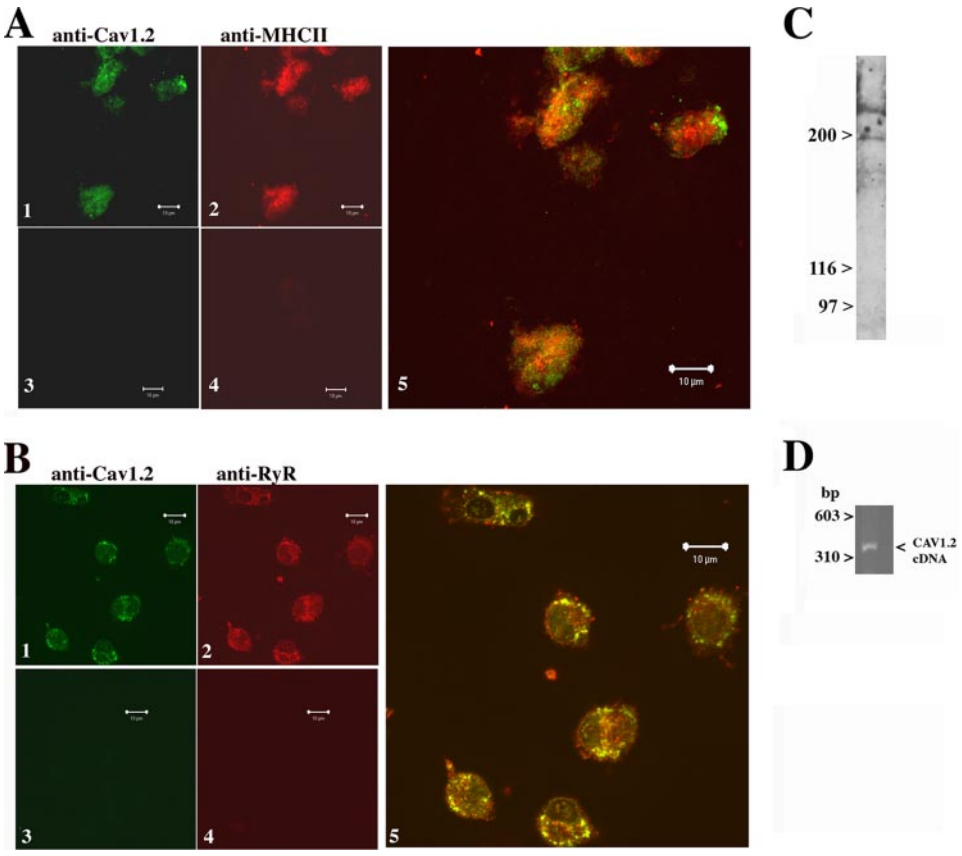


FIGURE 3. **$Ca_v1.2$ is expressed in iDCs and shows partial co-localization with the RyR.** *A*, immunofluorescence analysis on methanol fixed human iDCs. Shown are iDCs stained with rabbit anti-Cav1.2 polyclonal antibodies followed by Alexa Fluor-488-conjugated anti-rabbit IgGs (*1*) or Alexa Fluor-488 conjugated anti-rabbit IgGs alone (*3*) and mouse anti-MHC II (HLA DR) Abs followed by PE-conjugated goat anti-mouse Abs (*2*) or PE conjugate goat anti-mouse Abs alone (*4*). *Panel 5* shows the merged images, and *yellow-orange* pixels indicate overlapping fluorescent signal; *bars* indicate 10 $\mu$m. *B*, immunofluorescence analysis on acetone: methanol fixed-iDCs (*1*). iDCs stained with rabbit anti-$Ca_v1.2$ polyclonal antibodies followed by Alexa Fluor-488-conjugated anti-rabbit Abs or Alexa Fluor-488-conjugated anti-rabbit Abs alone (*3*) or goat anti-RyR polyclonal Ab followed by Alexa Fluor-555 conjugated anti-goat Abs (*2*) or Alexa Fluor-555 conjugate Abs alone (*4*). *Panel 5* shows the merged images, and *yellow-orange* pixels indicate overlapping fluorescent signals; *bars* indicate 10 $\mu$m. All images were acquired with a 100× Plan NEOFLUAR oil immersion objective (NA 1.3) mounted on a Zeiss Axiovert 100 confocal microscope. *C*, Western blot of total proteins of iDC ($1 \times 10^6$ cell/lane) separated on a 6% SDS polyacrylamide gel. The blot was incubated with rabbit anti-$Ca_v1.2$ followed by protein-G peroxidase. The immunoreaction was visualized by chemiluminescence. *D*, reverse transcription-PCR confirms the presence of the transcript for human $Ca_v1.2$ in iDC (see "Experimental Procedures" for details of the experimental conditions and primers used).

to amplify the human $Ca_v1.2$ transcript generated a band corresponding to the expected size (Fig. 3*D*) when amplifying cDNA. PCR amplification using primers specific for human $Ca_v1.1$ and $Ca_v1.3$ failed to amplify any band from cDNA of DCs (results not shown).

*Rapid Events Occurring after RyR1 Activation*—We were also interested in investigating if activation of the RyR1 leads to any direct changes in DCs. Immature DCs are extremely efficient at endocytosing (20, 21), so our first experiments were aimed at determining whether pretreatment of cells with a RyR1 agonist affects their capacity to endocytose FITC-labeled dextran. No difference in mean fluorescent intensity was observed between untreated iDCs or cells treated with 10 mM caffeine or 100 mM KCl. In 5 different experiments the mean ± S.E. % of FITC-positive cells was 98.5 ± 18.7% for cells pretreated with 100 mM KCl and 100% for iDCs ($p = 0.899$).

We next investigated whether RyR1 activation is linked to surface expression of MHC molecules. DCs express one pool of MHC class I molecules that are synthesized and loaded with antigenic peptides in the ER and two main populations of MHC class II molecules; one pool is synthesized *de novo* and is loaded with processed antigenic peptides in the ER, whereas the other is preformed and located within re-cycling endosomes (20). Immature dendritic cells were stimulated for 1–60 min with the RyR1 agonist caffeine, stained with anti-MHC I or anti-MHC II antibodies, and processed by flow cytometry. Fig. 4*A* shows that as early as 1 min after stimulation, there was a significant increase in surface fluorescence associated with MHC class II expression which then decayed back to resting levels after ~60 min of incubation at 37 °C. The increase in mean fluorescence intensity was reproducible and was specifically generated via DHPR-RyR1 signaling because (i) it also occurred after the addition of necrotic cell extracts and 100 mM KCl and (ii) the latter effects could be blocked by pretreatment of iDCs with dantrolene and nifedipine (Fig. 4*B*), (iii) it did not occur in cells treated with high levels (1 $\mu$g/ml) of LPS or with ATP, the latter agonist also generating a $Ca^{2+}$ signal, but via inositol 1,4,5-trisphosphate receptor activation (35), and (iv) KCl and necrotic extracts did not affect surface expression of MHC class I molecules (Fig. 4*C*). Such an effect may represent a specific and physiological pathway utilized by iDCs to rapidly express MHC class II molecules on their surface. The above-mentioned experiments were performed on "*in vitro*" generated DCs; when the same experiments were carried out on naturally occurring DCs isolated from mouse spleens, the addition of 100 mM KCl and necrotic cell extracts also caused a significant increase in surface expression of MHC class II molecules (Fig. 5*A*).

These findings are intriguing because of their rapid time course and because of their specificity but yield no information regarding their physiological role. We wondered whether the activation of the RyR1 signaling system could be important under specific conditions, namely when iDCs are present in an inflamed environment containing antigens as well as T cells. Notably, the classical pathways for T cell activation is via the inositol trisphosphate signaling pathway which leads to an increase in the $[Ca^{2+}]_i$ by releasing $Ca^{2+}$ from intracellular stores and by opening $Ca^{2+}$ channels on the plasma membrane (36). To compensate for the change in

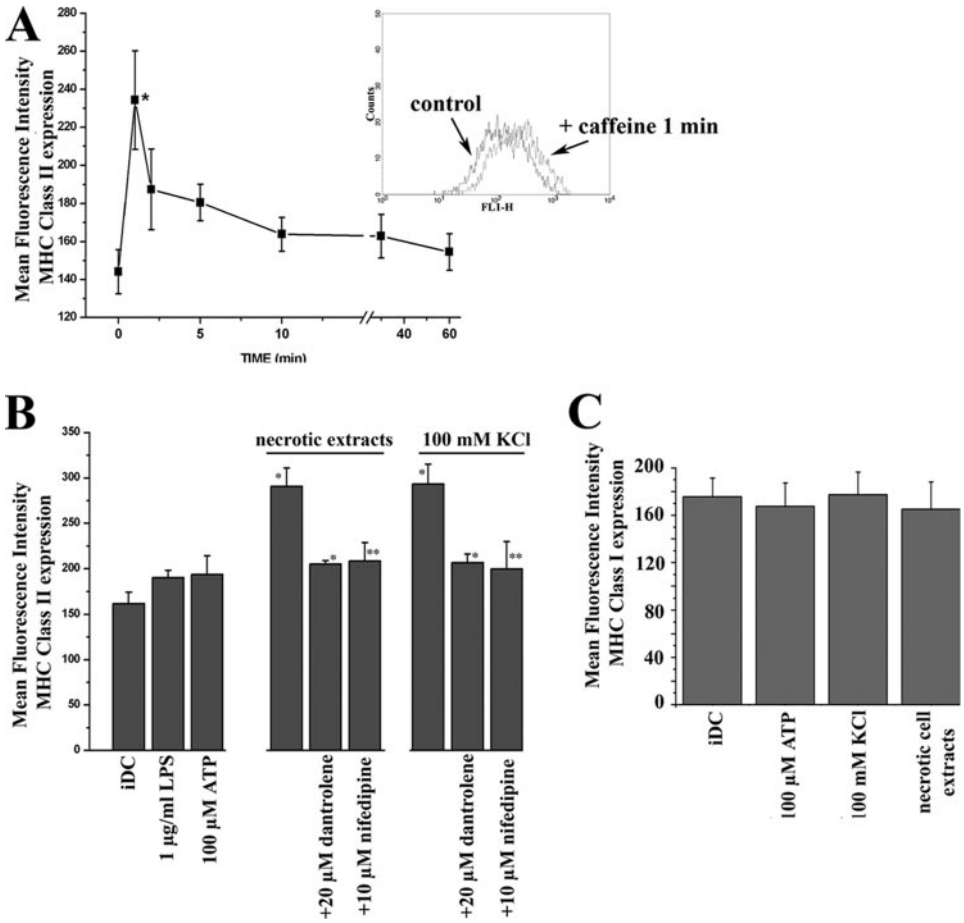


FIGURE 4. **Pharmacological activation of RyR induces a rapid increase in membrane-associated MHC class II molecules in iDC.** *A*, iDCs were treated with 10 mM caffeine for the indicated time, labeled with FITC-labeled anti-human HLA DR, fixed with paraformaldehyde, and analyzed by fluorescence-activated cell sorter as detailed under "Experimental Procedures." Results represent the mean fluorescent intensity (±S.E.) of four experiments carried out on different donors. *, $p < 0.015$. The *inset* shows a fluorescence-activated cell sorter histogram showing FITC fluorescence in immature DCs (*black line*) and in iDCs after the addition of 10 mM caffeine for 1 min (*gray line*). *B*, iDCs were treated for 1 min with the indicated substance and processed as described in *A*. Results represent the mean ± S.E. of 4–6 experiments. Significant differences were observed in the mean fluorescence intensity between iDCs and cells treated with necrotic cell extracts and between iDCs and cells treated with 100 mM KCl; significant differences in mean fluorescence intensity were observed between iDCs treated with necrotic cell extracts and KCl as compared with the mean fluorescence intensity of cells receiving similar treatments but preincubated with 10 μM nifedipine or 20 μM dantrolene; *, $p < 0.03$; **, $p < 0.05$. *C*, iDCs were treated for 1 min as indicated, labeled with FITC-labeled anti-human HLA A, B, C, and processed for fluorescence-activated cell sorter analysis as described for *A*. Results represent the mean fluorescence intensity (±S.E.) of five experiments carried out on different DC donors. Mean fluorescence intensity values were not significantly different in treated cells and iDC.

membrane potential caused by the $Ca^{2+}$ influx, $K^+$ channels (Kv1.3 and $K_{Ca}$) open, allowing efflux of $K^+$ ions out of the T cells, thus repolarizing the T cell membrane potential (37).

To determine whether these events (*i.e.* the $K^+$ efflux from T cells and DHPR-RyR1 activation in DCs) are functionally coupled *in vivo*, we studied if the direct interaction of antigen-specific T cells with DCs causes an increase in MHC II surface expression as well as an increase in the $[Ca^{2+}]_i$ of the DCs. To carry out the *in vivo* experiments, we exploited the fact that T lymphocytes from ABM $Rg^{-/-}$ mice express a transgenic T cell receptor which recognizes the class II MHC protein I-$A^{bm12}$ expressed on the surface of DCs from BM12Ly5.1 mice but not class II MHC protein I-$A^b$ expressed on the surface of control B6.Ly5.1 mice (24). CD11c-positive splenic DCs isolated from B6.Ly5.1 or BM12Ly5.1 mice were co-centrifuged with T cells from ABM $Rg^{-/-}$ mice and incubated an additional 5 min at 37 °C. Cells were then diluted with ice-cold PBS, stained with fluorescent Abs, and analyzed by flow cytometry. A further control consisting of T cells pretreated with charybdotoxin to block $K^+$ channels on T cells was also included. This toxin specifically blocks Kv1.3/$K_{Ca}$ channels at nM concentrations and inhibits $K^+$ efflux (25). When DCs from B6.Ly5.1 were incubated with T cells, there was an approximate 2.5-fold increase in the level of MHC class II molecules expressed on splenic DCs, indicating that co-centrifugation may non-specifically activate to a low extent both cell types. Interestingly, when BM12Ly5.1 DCs were co-centrifuged with untreated ABM $Rg^{-/-}$ T cells, there was a 5-fold increase in the level of MHC class II surface expression on splenic DCs (Fig. 5*B*). This 5-fold increase in class II MHC expression is specific as it was inhibited in the charybdotoxin-treated T cell group, supporting the idea that the full increase in MHC II expression is due to specific T cell $K^+$ channel opening occurring as a consequence of the T cell/DC interaction.

We used a similar approach to confirm that the interaction of BM12Ly5.1 DCs with ABM $Rg^{-/-}$ T cells causes a ryanodine-sensitive increase in the $[Ca^{2+}]_i$ of DCs. Fig. 5*C* shows a typical result obtained after the addition of ABM $Rg^{-/-}$ T cells to Fluo-4-loaded BM12DCs. As can be seen, the $[Ca^{2+}]_i$ of those DCs which were found to have T cells attached to them at the end of the experiment (*inset*, Fig. 5*C*) was found to increase in an oscillatory manner. This event was not synchronized in the responding cells as the moment of interaction between the two populations of cells was not coordinated. In line with our hypothesis, the increase in $[Ca^{2+}]_i$ induced by the BM12Ly5.1DC $Rg^{-/-}$ T cell interaction was most likely due to opening of $K^+$ channels on the T cells, as the $Ca^{2+}$ transients in the DCs were profoundly diminished after pretreatment of T cells with carybdotoxin (Fig. 5*D*). Finally, pretreatment of DCs with 500 μM ryanodine completely blocked the changes in $[Ca^{2+}]_i$ (Fig. 5*E*).

## DISCUSSION

In the present paper we investigated the signaling system involving the RyR in iDCs and show that the upstream events

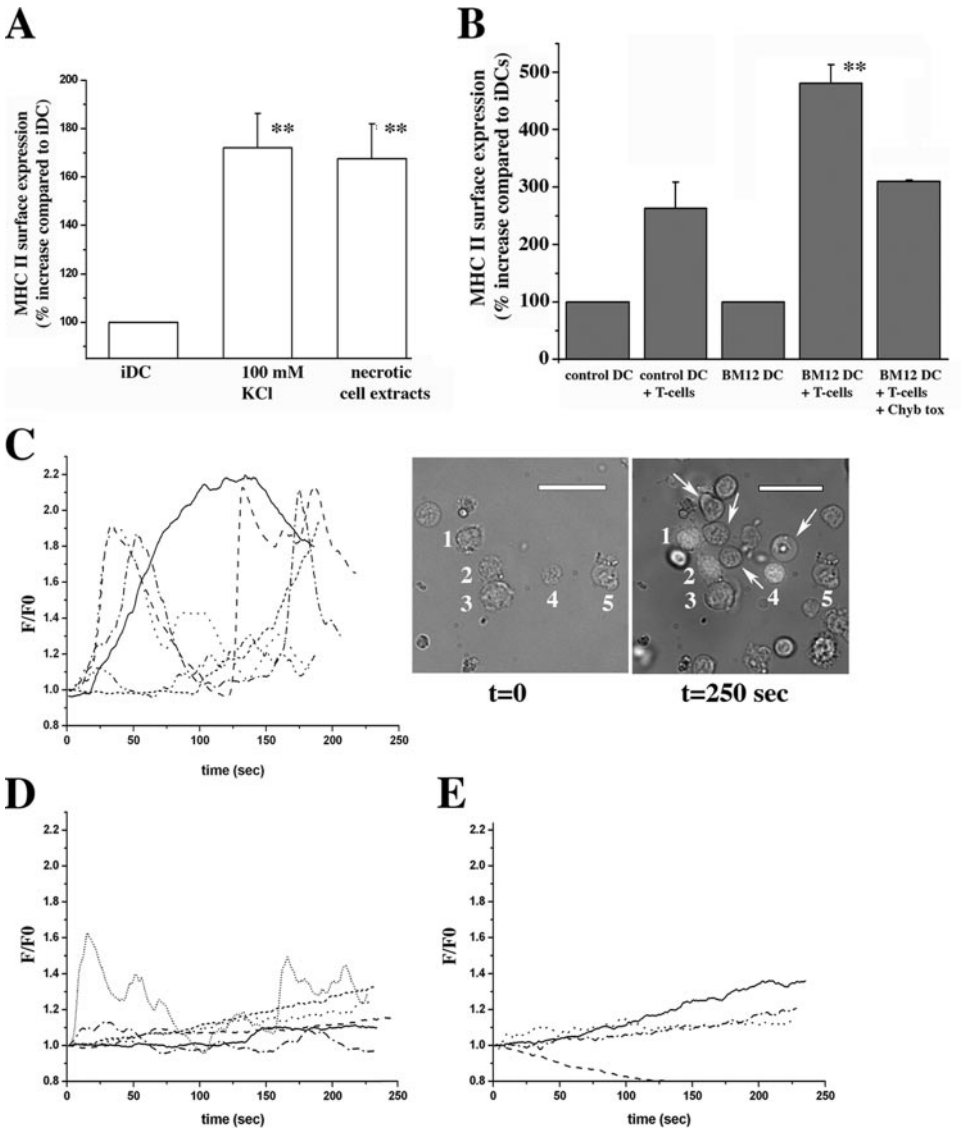


FIGURE 5. **Surface expression of MHC class II molecules is promoted by specific T cell-DC interaction or by KCl and necrotic cell extracts and is accompanied by an increase in the $[Ca^{2+}]_i$ in the DCs.** *A*, % induction in MHC II surface expression in CD11c-purified DCs isolated from mouse spleen cells after the addition of 100 mM KCl or necrotic cell extracts (mean % ± S.E., $n = 3–4$ experiments); **, $p < 0.007$. *B*, CD11c-positive dendritic cells were isolated from the spleens of either B6.C-H-2bm12Ly5.1 mice (BM12 DC) or B6.Ly5.1 mice (control DC) and co-centrifuged with T cells isolated from lymph nodes of ABM $Rg^{-/-}$ mice. T cells were either untreated or preincubated with 100 nM charybdotoxin (*Chyb tox*) for 45 min to block $K_v1.3$ and $IK_{Ca1}$ channels. After co-centrifugation, DC and T cells were incubated an additional 5 min at 37 °C. Cells were then diluted with ice-cold PBS, washed, and stained with FITC-labeled anti-mouse I-$A^b$ monoclonal antibody, biotin-labeled anti-mouse CD11c (Integrin $\alpha_x$ chain) monoclonal antibody, and PE-labeled anti-mouse CD45.1 monoclonal antibody. After selection of triple positive cells by fluorescence-activated cell sorter, MHC II expression was analyzed. Results are expressed as % increase in the mean fluorescent intensity compared with iDC (±S.E. of three experiments; **, $p < 0.007$). *C–E* show changes in the $[Ca^{2+}]_i$ in fluo-4 loaded BM12DC after the addition of ABM $Rg^{-/-}$ T cells. Experiments were performed as described under "Experimental Procedures." *C*, BM12DC + T cells. *D* is as in *C* except that T cells were preincubated with 100 nM charybdotoxin before addition to DCs. *E*, as in *C*, except DCs were incubated with 500 μM ryanodine during fluo-4 loading. Results are expressed as $F/F_0$ where $F$ is the fluorescent value at any given time, and $F_0$ is the initial fluorescence level obtained at time 0. Panels represent typical results obtained in six different experiments. *Insets* in *panel C* show brightfield photomicrograph of BM12DC at $t = 0$ and brightfield + epifluorescence of fluo-4-loaded BM12DC at the end of the experiment (250 s). *Numbers* indicate DCs that were analyzed and had T cells (*arrows*) adjacent to them. The *bar* indicates 10 μm.

leading to $Ca^{2+}$ release via the RyR1 are similar to those occurring in striated muscles and involve the functional interaction with the DHPR L-type $Ca^{2+}$ channel. We also show that RyR1 activation has direct and rapid physiological consequences leading to an increase in the level of MHC class II molecules on the surface of iDCs within seconds. Such a system may be important in the very early stages of an infection whereby prompt activation of the adaptive immune system could occur allowing rapid priming of T cells without having to wait for iDCs to undergo full functional maturation.

Although the expression of the RyR1 isoform in human and mouse dendritic cells has been clearly established (14, 16–17, 19), little information if any is available concerning its physiological mode of activation. In fact, RyRs are intracellular $Ca^{2+}$ channels localized on sarcoplasmic reticulum/ER membranes, and at least in excitable cells, their activation is coupled to DHPR L-type $Ca^{2+}$ channels present on the plasma membrane (3, 4). The latter channels have been characterized at the molecular, physiological, pharmacological, and biophysical level; they require strong depolarizing signals to open, can be blocked specifically by dihydropyridines and other organic $Ca^{2+}$ channel blockers, act as voltage sensors mediating $Ca^{2+}$ influx in response to membrane depolarization, and regulate a number of processes including muscle contraction, insulin secretion, neurotransmission, and gene transcription (4). DHPRs are macromolecular structures made up of four or five distinct subunits that are encoded by multiple genes. The α1 subunit constitutes the voltage sensor and the pore and usually associates with the β1 and α2δ subunits. Although DHPRs are predominantly expressed in excitable tissues such as neurons and muscle cells, pancreatic cells, and endocrine cells as well as T-lymphocytes have been shown to express the $Ca_v1.2$ isoform of L-type $Ca^{2+}$ channels (38–40).

In an early report Poggi *et al.* (33) showed that human DC express the β1 subunit of the DHPR as well an α subunit because they were stained with the fluorescent dihydropyridine analogue DM-BODIPY-DHP. They also demonstrated the involvement of DHPR-sensitive $Ca^{2+}$ channels in some DC functions such as apoptotic body engulfment and interleukin-12 production. We have extended these results and report that DCs have evolved a chi-

meric configuration, expressing the cardiac isoform of the $\alpha 1$ subunit (*i.e.* the $Ca_v1.2$ isoform), which functionally interacts with the skeletal isoform of the RyR. The first question arising is how can a functional coupling between the "cardiac" $Ca_v1.2$ isoform and the "skeletal" RyR1 isoform operate? In muscle cells depolarization of the plasma membrane is sensed by the $Ca_v1$, which acts as a voltage sensor activating the RyR to release $Ca^{2+}$ from intracellular stores. In skeletal muscle the $Ca_v1.1$ subunit and RyR1 interact directly (41–43), whereas in heart cells, which express type 2 RyR, the $Ca_v1.2$ subunit acts both as a voltage sensor and as a $Ca^{2+}$ channel, and the depolarizing signal allows $Ca^{2+}$ to flow into the cells from the extracellular environment (44). It is the influx of $Ca^{2+}$ which activates RyR2 through a mechanism of $Ca^{2+}$-induced $Ca^{2+}$ release. We suggest that in DCs, coupling between the DHPR and the RyR1 occurs as outlined in Fig. 9 of Schuhmeier *et al.* (45); membrane depolarization caused by an increase in $K^+$ is sensed by $Ca_v1.2$ present on the plasma membrane of DCs. Once activated, these channels allow $Ca^{2+}$ influx. In turn, this local increase in $[Ca^{2+}]_i$ in the DCs activates RyR1 through a $Ca^{2+}$ induced $Ca^{2+}$ release mechanism. Such a configuration is supported by the fact that RyR activation in DCs is strongly dependent on extracellular $Ca^{2+}$ and can be blocked by nifedipine. That this chimeric arrangement could function is supported by (i) the observation that electrical stimulation of dysgenic myotubes (which express RyR1 but lack endogenous DHPR), reconstituted with the cardiac $Ca_v1.2$, evokes myotube contraction albeit only in the presence of $Ca^{2+}$-containing medium (41) and (ii) by a report of Schuhmeier *et al.* (45) who showed that different $Ca_v$ channel isoforms (1.1, 1.2, and 2.1) can functionally interact with RyR1.

The most intriguing questions arising from the observation that DCs express DHPRs are how and when would these voltage-sensor-activated $Ca^{2+}$ channels be activated physiologically? Indeed DCs are not typically classified as electrically excitable cells, yet we show that the addition of either necrotic cell extracts or KCl both cause (i) plasma membrane depolarization, (ii) nifedipine-sensitive increase in $[Ca^{2+}]_i$, and (iii) rapid and nifedipine-sensitive increase in surface expression of MHC class II molecules. Necrotic and dying cells are present in any tissue after extensive injury due to physical or mechanical traumas, inflammation, or infections, and they can release a number of factors and proteins including uric acid crystals, nuclear-mobility group box 1 protein, and heat shock proteins (HSP96, -90, -70 and calreticulin) which can all induce DC maturation (46–48). In addition, because the intracellular $K^+$ concentration is ~140 mM, dying cells will necessarily release $K^+$ ions into the extracellular medium; our results support the hypothesis that necrotic cells may lead to activation of the DHPR-RyR signaling pathway by releasing a number of factors, including $K^+$. This is supported by the finding that necrotic extracts passed through a 0.22-$\mu$m filter caused a nifedipine-and ryanodine-sensitive increase in the $[Ca^{2+}]_i$ as well as membrane depolarization, but extracts dialyzed against PBS using a 3000-kDa cut-off membrane did not alter the membrane potential. Because ions would be removed by dialysis, these data suggest that $K^+$ released from the dead cells may be physiologically involved in the *in vivo* activation of the DHPR-RyR1 signaling pathway.

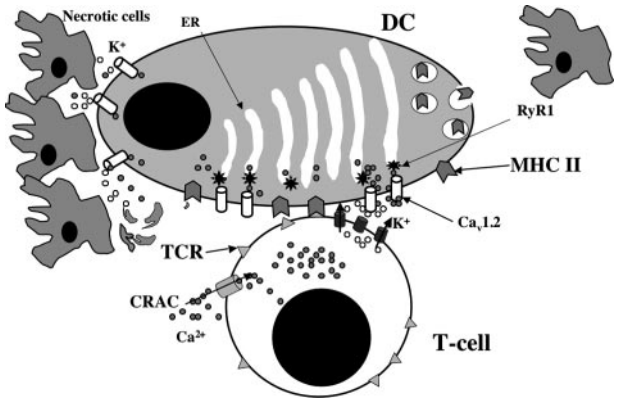


FIGURE 6. **Schematic depicting the model of RyR1-dependent signaling pathways in DC.** KCl released from dead cells in the vicinity of DCs causes membrane depolarization, which is sensed by the DHPR voltage sensor. Alternatively, interaction of T cells with iDC, strong enough to activate an increase in the $[Ca^{2+}]_i$ via release from intracellular stores and activation of $Ca^{2+}$ influx, is accompanied by efflux of $K^+$ to repolarize the T cell membrane potential. This $K^+$ is released onto the iDCs and can be sensed by the DHPR. This leads to activation of the RyR1 signaling pathway causing the rapid expression of MHC class II molecules onto the surface of iDCs. The latter molecules could be loaded with antigenic peptides and interact *in situ* with T cells to initiate an early and rapid specific immune response. *TCR*, T cell receptor; *CRAC*, $Ca^{2+}$ release activated $Ca^{2+}$ channel.

Another important question is whether the DHPR-RyR1 signaling pathway is only involved in the generation of co-stimulatory signals leading to DC maturation or whether it can rapidly and directly activate specific functions. Our results exclude that endocytosis, a process intimately connected with iDC function, and expression of MHC class I molecules on the plasma membrane are influenced by activation of the RyR signaling pathway. On the other hand, our results show that surface expression of MHC class II molecules is rapidly (within seconds) and significantly increased by the activation of the RyR1 signaling pathway. DCs synthesize large quantities of MHC class II molecules which classically bind peptides derived from endocytosed proteins and present them on their surface for interaction with T cells to initiate a specific immune response. They also express empty MHC II molecules on their surface as well as sequestered MHC class II molecules within intracellular compartments (22, 49). These sequestered molecules apparently reside unproductively within the cell. The results of the present study indicate that activation of the DHPR-RyR1 pathway causes expression of preformed MHC class II molecules on the surface of DCs. Empty surface MHC II molecules can be loaded with antigenic peptides from the extracellular medium, allowing even immature DCs to present peptides to T cells without intracellular processing (50, 51). We hypothesize that RyR1 activation in DCs leads to the rapid surface expression of sequestered MHC II molecules. This would be particularly important for iDC and T cells to interact efficiently directly in an inflamed tissue where dead or dying cells are present, leading to the rapid amplification of a specific immune response. Such a rapid activation must be strictly controlled and most likely requires T cells and iDCs to generate orthograde and retrograde signals, which would strengthen the intracellular signals generated and lead to T cell-dependent immune responses. That T cells are capable of releasing soluble factors which trigger DCs is substantiated by our findings that

the direct interaction of murine T cells with a transgenic T cell receptor specific for the I-$A^{bm12}$ protein and BM12Ly5.1DC (which express the I-$A^{bm12}$) causes (i) a 5-fold increase in surface expression of MHC class II molecules and (ii) an increase in the $Ca^{2+}$ in the DCs which is sensitive to high concentrations of ryanodine, which inactivate the RyR $Ca^{2+}$ channel (30, 31), and charybdotoxin, which blocks $K^+$ channels on T cells. We suggest that the increase in MHC II surface expression is promoted by efflux of $K^+$ via channels present on the surface of T cells which open after the increase in $[Ca^{2+}]_i$ triggered by engagement of the T cell receptor. This idea is supported by the observation that up-regulation of MHC II could be blocked by pretreatment of T cells with the $K^+$ channel toxin charybdotoxin. A schematic outlining this hypothesis is depicted in Fig. 6.

In conclusion we present evidence that the DHPR-RyR1 signaling machinery plays an important role in up-regulation of MHC class II molecules on the surface of DCs, and this signaling pathway could be an important target for drugs aimed at improving the immune system by increasing the efficiency of antigen presentation or at impairing the immune system by decreasing presentation of autoantigens responsible for the induction of autoimmune disorders.

*Acknowledgments—We acknowledge the support of the Departments of Anesthesia and Surgery of the Basel University Hospital. We thank Prof. Ed Palmer for supplying the B6.C-H-2bm12Ly5.1, B6.Ly5.1, and ABM $Rg^{-/-}$ mice and for constructive suggestions, Prof. Isaac Pessoh for helpful suggestions, Prof. Gennaro DeLibero for helpful discussion, and Natalia Gomez-Ospina and Prof. Ricardo Dolmetsch for providing the purified anti-$Ca_v$1.2 (anti-CCAT) antibodies.*

## REFERENCES


1. Berridge, M. J., Lipp, P., and Bootman, M. D. (2000) *Nat. Rev. Mol. Cell Biol.* **1,** 11–21
2. Berridge, M., Bootman, M. D., and Roderick, H. L. (2003) *Nat. Rev. Mol. Cell Biol.* **4,** 517–529
3. Catterall, W. A. (2000) *Annu. Rev. Cell Dev. Biol.* **16,** 521–555
4. Catterall, W. A., Perez-Reyes, E., Snutch, T. P., and Striessnig, J. (2005) *Pharmacol. Rev.* **57,** 411–425
5. Sutko, J. L., and Airey, J. A. (1996) *Physiol. Rev.* **76,** 1027–1071
6. Franzini-Armstrong, C., and Protasi, F. (1997) *Physiol. Rev.* **77,** 699–729
7. Bers, D. M. (2004) *J. Mol. Cell. Cardiol.* **37,** 417–429
8. Treves, S., Anderson, A. A., Ducreux, S., Divet, A., Bleunven, C., Grasso, C., Paesante, S., and Zorzato, F. (2005) *Neuromuscul. Disord.* **15,** 577–587
9. Robinson, R., Carpenter, D., Shaw, M. A., Halsall, J., and Hopkins, P. (2006) *Hum. Mutat.* **27,** 977–989
10. Wehrens, X. H., and Marks, A. R. (2003) *Trends Biochem. Sci.* **28,** 671–678
11. George, C. H., Jundi, H., Thomas, N. L., Fry, D. L., and Lai, F. A. (2007) *J. Mol. Cell. Cardiol.* **42,** 34–50
12. Tarroni, P., Rossi, D., Conti, A., and Sorrentino, V. (1997) *J. Biol. Chem.* **272,** 19808–19813
13. Hosoi, E., Nishizaki, C., Gallagher, K. L., Wyre, H. W., Matsuo, Y., and Sei, Y. (2001) *J. Immunol.* **167,** 4887–4894
14. O'Connell P. J., Klyachko, V. A., and Ahern, G. P. (2002) *FEBS Lett.* **512,** 67–70
15. Ducreux, S., Zorzato, F., Ferreiro, A., Jungbluth, H., Muntoni, F., Monnier, N., Müller, C. R., and Treves, S. (2006) *Biochem. J.* **395,** 259–266
16. Goth, S. R., Chu, R. A., Gregg, J. P., Cjerednichenko, G., and Pessah, I. N. (2006) *Environ. Health Perspect.* **114,** 1083–1091
17. Bracci, L., Vukcevic, M., Spagnoli, G., Ducreux, S., Zorzato, F., and Treves, S. (2007) *J. Cell Sci.* **120,** 2232–2240
18. Sei, Y., Gallagher, K. L., and Basile, A. S. (1999) *J. Biol. Chem.* **274,** 5995–6002
19. Uemura, Y., Liu, T. Y., Narita, Y., Suzuki, M., Ohshima, S., Mizukami, S., Ichihara, Y., Kikuchi, H., and Matsushita, S. (2007) *Biochem. Biophys. Res. Commun.* **362,** 510–515
20. Trombetta, S. E., and Mellman, I. (2005) *Annu. Rev. Immunol.* **23,** 975–1028
21. Lanzavecchia, A. (1996) *Curr. Opin. Immunol.* **8,** 348–354
22. Cella, M., Engering, A., Pinet, V., Pieters, J., and Lanzavecchia, A. (1997) *Nature* **388,** 782–787
23. Dauer, M., Obermaier, B., Herten, J., Haerle, C., Pohl, K., Rothenfusser, S., Schnurr, M., Endres, S., and Eigler, A. (2003) *J. Immunol.* **170,** 4069–4076
24. Bäckström, B. T., Müller, U., Hausmann, B. T., and Palmer, E. (1998) *Science* **281,** 835–838
25. Chandy, G. K., Wulff, H., Beeton, C., Pennington, M., Gutman, G. A., and Cahalan, M. D. (2004) *Trends Pharmacol. Sci.* **25,** 280–289
26. Sauter, B. B., Albert, M. L., Francisco, L., Larsson, M., Somersan, S., and Bhardwaj, N. (2000) *J. Exp. Med.* **191,** 423–433
27. Zhou, L. J., and Tedder, T. F. (1996) *Proc. Natl. Acad. Sci. U. S. A.* **93,** 2588–2592
28. Lachmann M., Berchtold S., Hauber, J., and Steinkasserer, A. (2002) *Trends Immunol.* **23,** 273–275
29. Zhao, F., Li, P., Chen, S. R., Louis, C. F., and Fruen, B. R. (2001) *J. Biol. Chem.* **276,** 13810–13816
30. Meissner, G. (1986) *J. Biol. Chem.* **261,** 6300–6306
31. Zimanyi, I., Buck, J., Abranson, J. J., Mack, M. M., and Pessah, I. (1992) *Mol. Pharmacol.* **42,** 1049–1067
32. Kwan, C. Y., Takemura, H., Obie, J. F., Thastrup, O., and Putney, J. W., Jr. (1990) *Am. J. Physiol.* **258,** C1006–C1015
33. Poggi, A., Rubartelli, A., and Zocchi, R. (1998) *J. Biol. Chem.* **273,** 7205–7209
34. Gomez-Ospina, N., Tsuruta, F., Barreto-Chang, O., Hu, L., and Dolmetsch, R. (2006) *Cell* **127,** 591–606
35. Ralevic, R., and Burnstock, G. (1998) *Pharmacol. Rev.* **50,** 413–455
36. Lewis, R. S. (2001) *Annu. Rev. Immunol.* **19,** 497–521
37. Panyi, G., Varga, Z., and Gaspar, R. (2004) *Immunol. Lett.* **92,** 55–66
38. Vignali, S., Leiss, V., Karl, R., Hofmann, F., and Welling, A. (2006) *J. Physiol.* (*Lond.*) **572,** 691–706
39. Sedej, S., Tsujimoto, T., Zorec, R., and Rupnik, M. (2004) *J. Physiol.* (*Lond.*) **555,** 769–782
40. Badou A., Jha, M. K., Matza, D., Mehal, W. Z., Freichel, M., Flockerzi, V., and Flavell, R. A. (2006) *Proc. Natl. Acad. Sci. U. S. A.* **103,** 15529–15534
41. Tanabe, T., Beam, K. G., Adams B. A., Niidome, T., and Numa, S. (1990) *Nature* **346,** 567–569
42. Nakai, J., Tanabe, T., Konno, T., Adams, B., and Beam, K. G. (1998) *J. Biol. Chem.* **273,** 24983–24986
43. Grabner, M., Dirksen, R. T., Suda, N., and Beam, K. G. (1999) *J. Biol. Chem.* **274,** 21913–21919
44. Näbauer, M., Callewaert, G., Cleemann, L., and Morad, M. (1989) *Science* **244,** 800–803
45. Schuhmeier, R. P., Goudadon, E., Ursu, D., Kaseielke, N., Flucher, B. E., Grabner, M., and Melzer, W. (2005) *Biophys. J.* **88,** 1765–1777
46. Basu, S., Binder, R. J., Suto, R., Anderson, K. M., and Srivastava, P. K. (2000) *Int. Immunol.* **12,** 1539–1546
47. Shi, Y., Evans, J. E., and Rock, K. L. (2003) *Nature* **425,** 516–521
48. Rovere-Querini, P., Capobianco, A., Scaffidi, P., Valentinis, B., Catalanotti, F., Giazzon, M., Dumitriu, I. E., Müller, S., Iannacone, M., Traversari, C., and Bianchi, M. E. (2004) *EMBO Rep.* **5,** 825–830
49. Chow, A., Toomre, D., Garrett, W., and Mellman, I. (2002) *Nature* **418,** 988–994
50. Santambrogio, L., Sato, A. K., Fischer, F. R., Dorf, M. E., and Stern, L. J. (1999) *Proc. Natl. Acad. Sci. U. S. A.* **96,** 15050–15055
51. Santambrogio, L., Sato, A. K., Carven, G. J., Belyasnkaya, S. L., Strominger, J. L., and Stern, L. J. (1999) *Proc. Natl. Acad. Sci. U. S. A.* **96,** 15056–15061

# Ryanodine Receptor Activation by $Ca_V1.2$ Is Involved in Dendritic Cell Major Histocompatibility Complex Class II Surface Expression

Mirko Vukcevic, Giulio C. Spagnoli, Giandomenica Iezzi, Francesco Zorzato and Susan Treves

*J. Biol. Chem. 2008, 283:34913-34922.*
*doi: 10.1074/jbc.M804472200 originally published online October 16, 2008*

---